

# UC Davis

## UC Davis Previously Published Works

### Title

Galectin-1 inhibition induces cell apoptosis through dual suppression of CXCR4 and Ras pathways in human malignant peripheral nerve sheath tumors

### Permalink

<https://escholarship.org/uc/item/9kc079zr>

### Journal

Neuro-Oncology, 21(11)

### ISSN

1522-8517

### Authors

Shih, Tsung-Chieh

Fan, Yunpeng

Kiss, Sophie

et al.

### Publication Date

2019-11-04

### DOI

10.1093/neuonc/noz093

Peer reviewed

# Galectin-1 inhibition induces cell apoptosis through dual suppression of CXCR4 and Ras pathways in human malignant peripheral nerve sheath tumors

Tsung-Chieh Shih<sup>®</sup>, Yunpeng Fan, Sophie Kiss, Xiaocen Li, Xiaojun Nicole Deng, Ruiwu Liu, Xiao-Jia Chen, Randy Carney, Amanda Chen, Paramita M. Ghosh, and Kit S. Lam

*Department of Biochemistry and Molecular Medicine, University of California Davis, Sacramento, California, USA (T.-C.S., S.K., X.L., X.N.D., R.L., R.C., A.C., P.M.G., K.S.L.); College of Veterinary Medicine, Northwest A&F University, Yangling, Shaanxi, P R China (Y.F.); Institute of Biomedicine & Cell Biology Department, Jinan University, National Engineering Research Center of Genetic Medicine, Guangdong Provincial Key Laboratory of Bioengineering Medicine, and Guangdong Provincial Engineering Research Center of Biotechnological Medicine, Guangdong, Guangzhou, China (X.-J.C.); Department of Urology, University of California Davis, Sacramento, California, USA (P.M.G.); VA Northern California Health Care System, Sacramento, California, USA (P.M.G.); UC Davis NCI Designated Comprehensive Cancer Center, University of California Davis, Sacramento, California, USA (K.S.L.)*

**Corresponding Authors:** Tsung-Chieh Shih and Kit S. Lam, Department of Biochemistry & Molecular Medicine, University of California at Davis, Suite 2301, 2700 Stockton Blvd, Sacramento, CA 95817 ([tcshih@ucdavis.edu](mailto:tcshih@ucdavis.edu) and [kslam@ucdavis.edu](mailto:kslam@ucdavis.edu)).

## Abstract

**Background.** The Ras signaling pathway is commonly dysregulated in human malignant peripheral nerve sheath tumors (MPNSTs). It is well known that galectin-1 (Gal-1) is essential to stabilize membrane Ras and thereby induce the activation of Ras. However, the role of Gal-1 in MPNST progression remains unknown. The aim of this study was to examine whether Gal-1 knockdown could have an effect on the Ras signaling pathway.

**Methods.** Cell viability, apoptosis assay, and colony formation were performed to examine the effects of inhibition of Gal-1 in MPNST cells. We used a human MPNST xenograft model to assess growth and metastasis inhibitory effects of Gal-1 inhibitor LLS2.

**Results.** Gal-1 was upregulated in MPNST patients and was highly expressed in MPNST cells. Knockdown of Gal-1 by small interfering (si)RNA in Gal-1 expressing MPNST cells significantly reduces cell proliferation through the suppression of C-X-C chemokine receptor type 4 (CXCR4) and the rat sarcoma viral oncogene homolog (RAS)/extracellular signal-regulated kinase (ERK) pathway, which are important oncogenic signaling in MPNST development. Moreover, Gal-1 knockdown induces apoptosis and inhibits colony formation. LLS2, a novel Gal-1 allosteric small molecule inhibitor, is cytotoxic against MPNST cells and was able to induce apoptosis and suppress colony formation in MPNST cells. LLS2 treatment and Gal-1 knockdown exhibited similar effects on the suppression of CXCR4 and RAS/ERK pathways. More importantly, inhibition of Gal-1 expression or function by treatment with either siRNA or LLS2 resulted in significant tumor responses in an MPNST xenograft model.

**Conclusion.** Our results identified an oncogenic role of Gal-1 in MPNST and that its inhibitor, LLS2, is a potential therapeutic agent, applied topically or systemically, against MPNST.

## Key Point

1. Targeting Gal-1 by siRNA or Gal-1 inhibitor LLS2 impairs MPNST progression.

## Importance of the Study

MPNST is a malignant tumor with a fairly poor prognosis (5-year survival of <50%) and is a leading cause of increased death for neurofibromatosis type 1 patients. Surgery to remove neurofibromas is the main treatment for MPNST. For unresectable or metastatic diseases, chemotherapeutic drugs are only marginally effective. However, there are no effective systemic therapies for MPNST patients. Ras signaling pathway is commonly dysregulated in MPNST patients. Ras pathway and downstream effectors are

implicated in the pathogenesis of MPNST. Here we show that Gal-1 was upregulated in MPNST. Our preclinical data demonstrate that inhibition of Gal-1 expression or function by treatment with either siRNA or LLS2 resulted in significant tumor responses in an MPNST xenograft model. Given these results, we reason that Gal-1 is an excellent therapeutic target against MPNST and that LLS2 is an excellent lead compound for the development of novel therapeutics against MPNST.

Neurofibromatosis type 1 (NF1) is the most common form of neurofibromatosis, which affects about 100,000 Americans. The most common nerve-associated tumors in NF1 are neurofibromas, which are mostly benign and broadly classified into dermal and plexiform subtypes. Although neurofibromas are benign tumors, plexiform neurofibromas can undergo transformation into malignant peripheral nerve sheath tumors (MPNSTs), which have a fairly poor prognosis (5-year survival of <50%) and are a leading cause of death for NF1 patients.<sup>1</sup> Unfortunately, there is no effective treatment for this disease. There is great clinical need to develop novel, efficacious, and less toxic topical and systemic medical treatment against this debilitating disease.<sup>2</sup>

Galectin-1 (Gal-1), a 14 kDa lectin, is a member of a family of galectins with an affinity for  $\beta$ -galactosides. Gal-1, in its dimeric form, is involved in the regulation of proliferation, apoptosis, cell cycle, and angiogenesis. Its level is elevated in many other human cancers (ovarian,<sup>3</sup> prostate,<sup>4</sup> lung,<sup>5</sup> breast,<sup>6</sup> kidney,<sup>7</sup> and pancreatic cancer<sup>8</sup>). Mechanistically, Gal-1 is known to stabilize activated H-Ras (G12V) at the plasma membrane, which is essential for induction of the rat sarcoma viral oncogene homolog (RAS)/extracellular signal-regulated kinase (ERK) oncogenic signaling pathway.<sup>9</sup> In addition, elevated RAS/mitogen-activated protein kinase (MAPK) activity is found in neurofibroma and MPNST cells derived from NF1 patients, due to the loss of function of neurofibromin, which is a negative regulator of Ras.<sup>10–12</sup> These results indicate that inhibition of Gal-1 function is a promising therapeutic approach against NF1-associated neurofibroma and MPNST.

In addition to neurofibromin, elevated C-X-C chemokine receptor type 4 (CXCR4) has previously been reported to promote MPNST tumor progression.<sup>13</sup> CXCR4/CXC ligand 12 triggers the activation of phosphatidylinositol-3 kinase and  $\beta$ -catenin signaling to stimulate cyclin D1 expression and cell-cycle progression. The CXCR4 antagonist AMD3100 has growth-inhibitory effects on primary cultured mouse and human MPNST cells, tumor allografts, and spontaneous genetically engineered mouse models of MPNST. Thus, inhibition of CXCR4 expression could suppress MPNST growth. However, the molecular mechanisms that regulate CXCR4 expression in MPNST are still unknown.

In our previous study, we developed the one-bead two-compound (OB2C) screening method, which is a highly efficient drug screening platform.<sup>14</sup> Through this screening

platform, we have recently identified a benzimidazole small-molecule compound, LLS2, as a pro-apoptotic agent and potent Gal-1 inhibitor. Binding of LLS2 to Gal-1 decreased membrane-associated H-Ras and K-Ras and contributed to the suppression of the RAS/ERK pathway. LLS2 can cause apoptosis in colon, pancreatic, ovarian, prostate, and breast cancer cells and inhibit the tumor growth in ovarian cancer xenografts.<sup>14</sup>

In this study, we found that upregulation of Gal-1 plays a crucial role in CXCR4 and RAS/ERK pathways for MPNST. Knockdown of Gal-1 by siRNA or treatment with LLS2 effectively induces apoptosis in MPNST cells, and inhibits the growth of MPNST cell lines in vitro and in vivo. Given these results, we reason that Gal-1 is an excellent therapeutic target against MPNST, and that LLS2 is an excellent lead compound for the development of novel therapeutics against MPNST.

## Materials and Methods

### Analysis of Gal-1 Expression in Human Neurofibroma and MPNST

Human peripheral nerve tumor tissue array was obtained from US Biomax (SO1001a). The detailed procedure of immunohistochemistry is described in our published study.<sup>15</sup> The expression of *LGALS1*, *CXCR4*, and *NF1* in MPNST and neurofibroma was identified from the Oncomine database (<https://www.oncomine.org/resource/login.html>). Datasets were generated from the studies by Henderson<sup>16</sup> and Nakayama.<sup>17</sup> *LGALS1*, *CXCR4*, and *NF1* are expressed relative to housekeeping genes in MPNST and neurofibroma. All data are log transformed and median centered per array.

### Cell Lines

Normal human schwann cells (huSC) were purchased from ScienCell. MPNST-derived cell lines sNF02.2 (*NF1*<sup>+/−</sup>) and sNF96.2 (*NF1*<sup>−/−</sup>) were purchased from American Type Culture Collection. HuSC was maintained in human Schwann cell medium (ScienCell). MPNST sNF02.2 and sNF96.2 cells were maintained in Dulbecco's modified Eagle's medium supplemented with 10% fetal bovine serum and 1% penicillin/streptomycin, and grown in 5% CO<sub>2</sub> at 37°C. Mycoplasma testing was routinely performed every month.

## Plasmids and Gene Knockdown

NF96.2 and NF2.2 cells were seeded on 6-well plates. Two small interfering (si)RNAs targeting the different region of *LGALS1* mRNA were used to decrease Gal-1 expression (siGal-1 #1: HSS106025 [Invitrogen] and siGal-1 #2: s194592 [Ambion]). Cells were transfected with 40 nM negative control mimic or mixed siRNA against Gal-1 using Lipofectamine 2000 transfection reagent (Life Technologies) according to the manufacturer's instructions. NF96.2 cells were transfected with 1  $\mu$ g control (sc-108060, Santa Cruz) or Gal-1 short hairpin (sh)RNA plasmid (sc-35441-SH, Santa Cruz) or pcDNA-H-Ras or pcDNACXCR4. Cell lysates were collected at 72 h after transfection and subject to immunoblotting to check protein expression.

## Cell Viability and Apoptosis Assay

For cell viability,  $5 \times 10^3$  NF96.2 and NF2.2 cells were seeded into 96-well plates per well. Cells were allowed to attach for 24 h prior to drug treatment for 72 h. After 24 h, medium was removed and the cells were treated with the indicated concentrations of LLS2 or siRNA. Ten millimolar LLS2 stock solutions (100X) were prepared in 100% dimethyl sulfoxide (DMSO); 10 mM LLS2 was diluted 1:100 with cell culture medium to produce 100  $\mu$ M LLS2 in 1% DMSO, and then was two-fold serially diluted in cell culture medium. After the indicated timepoints, cell viability was determined by assay by MTT (3-(4,5-dimethylthiazol-2-yl)-2,5-diphenyltetrazolium bromide). For apoptosis assay, caspase-3/7 activity was measured after treatment with 0.25% DMSO or 25  $\mu$ M LLS2 or siRNA for 72 h by using a luminescent caspase-Glo 3/7 assay kit (Promega). Early apoptosis was detected using the fluorescein isothiocyanate annexin-V Apoptosis Detection Kit (BD Biosciences).

## Ras Activation Assay

Activated Ras was detected using the Ras Activation Assay Kit (17–218, Millipore) according to the manufacturer's instructions. Briefly, shRNA transfected or LLS2 treated cells were lysed and Raf-1 Ras-binding domain (RBD) agarose beads were added to 200  $\mu$ g cell lysates for 30 min at 4°C followed by centrifugation at 14000x *g* for 10 s at 4°C. After washing, the agarose-bound Ras was incubated in 2X Laemmli reducing sample buffer (126 mM Tris/HCl, 20% glycerol, 4% sodium dodecyl sulfate [SDS], 0.02% bromophenol blue), which will subsequently be resolved on SDS-polyacrylamide gel electrophoresis (PAGE) and detected by western blotting with an anti-Ras antibody (05-516, Millipore).

## Immunoblotting Analysis

Cells were lysed in a radioimmunoprecipitation assay buffer (50 mM Tris-HCl pH 7.5, 0.5% sodium deoxycholate, 1% NP-40 [nonyl phenoxyethoxyethanol], 0.1% SDS, 150 mM NaCl, 2 mM EDTA, 50 mM NaF, 1 mmol/L dithiothreitol, 2 mg/mL aprotinin, and 2 mg/mL leupeptin)<sup>14</sup> and incubated on ice for 20 min. After centrifugation at

12000x *g* for 20 min at 4 °C, total cell lysates were collected and quantified by bicinchoninic acid assay. Twenty micrograms of each lysate was boiled in 2X Laemmli SDS-PAGE sample buffer (126 mM Tris/HCl, 20% glycerol, 4% SDS, 0.02% bromophenol blue) at 95°C for 10 min, followed by separation on 12% SDS-PAGE gels and transference to polyvinylidene difluoride membrane (Bio-Rad). After blocking with 10% nonfat dried milk in Tris-buffered saline (20 mM Tris pH 7.5, 150 mM NaCl) for 1 h, the membrane was incubated with the specific primary antibodies against Nf1, CXCR4, phospho-MEK (Ser217/221), MEK, phospho-ERK(Thr202/Tyr204), ERK, or beta-actin (14623, 97680, 9154, 8727, 4377, 9107, 3700, Cell Signaling) at 4°C overnight. The membrane was washed in TBS-T (20 mM Tris pH 7.5, 150 mM NaCl, 0.1% Tween 20) three times. The membranes of CXCR4, phospho-MEK (Ser217/221), MEK, and phospho-ERK(Thr202/Tyr204) were incubated with anti-rabbit immunoglobulin G (IgG) horseradish peroxidase (HRP)-linked secondary antibody (7074, Cell Signaling) at 37°C for 1 h. The ERK and beta-actin membranes were incubated with anti-mouse IgG HRP-linked secondary antibody (7076, Cell Signaling) at 37°C for 1 h. After washing with TBS-T 3 times, electrochemiluminescence substrate (Amersham) was added and chemiluminescence signal was detected by a charge-coupled device camera (Bio-Rad).

## Colony Formation Assays

Five hundred NF96.2 cells transfected with shRNA targeting control or Gal-1 were seeded into 24-well ultra-low attachment plates (Corning). The growth medium was replaced every 3 days. The colonies were formed after 2 weeks and then treated with 0.25% DMSO or 25  $\mu$ M LLS2. Colonies were imaged for colony size calculation 5 days post treatment. Colony diameter larger than 50  $\mu$ m was counted manually from 3 different wells.

## In Vivo Xenograft Tumor Assays

The Institutional Animal Care and Use Committee of the University of California Davis approved animal experiments in this study. LLS2 stock solutions (6X) were prepared in 50% absolute alcohol and 50% cremophor to make 15 mg/mL. Prior to administration, each was diluted with saline to produce 2.5 mg/mL solutions. Female congenital athymic Bagg albino/c nude (nu/nu) mice were purchased from The Jackson Laboratory. Resuspended in 100  $\mu$ L of 50% Matrigel (BD Biosciences) were  $5 \times 10^6$  NF96.2 cells constitutively expressing luciferase, which were subcutaneously injected into the right side of the mouse dorsal flank. After 12 weeks implantation, the tumors were formed (~75 mm<sup>3</sup>). Mice were randomly divided into control and treatment groups, with 6 mice per group. Mice were given a vehicle 8.7% alcohol/8.7% cremophor or 25 mg/kg LLS2 daily i.v. administration for 5 successive days. Three weeks after treatment, mice were sacrificed and tumors were excised and weighed. For lung metastasis model, luciferase-tagged NF96.2 cells were intravenously injected into nude mice, followed by LLS2 treatment (15 mg/kg once daily for 5 days) 3 weeks later. After 12 weeks implantation, bioluminescence

signals were detected by the IVIS 200 Imaging System (Caliper LifeSciences), 5 min after intraperitoneal injection of 100 mg/kg D-luciferin.

### Statistical Analysis

Expression level of Gal-1 was scored as follows: 0, negative; 1, low intensity; 2, moderate intensity; 3, high intensity; and 4, very high intensity. Two pathologists have visually scored immunohistochemistry data. All in vitro studies were performed in triplicate in 3 different experiments. Two-tailed Student's *t*-test was used for comparison between variables. All results were expressed as mean  $\pm$  SD and a *P*-value  $<0.05$  was considered statistically significant.

## Results

### Gal-1 Expression in Human MPNST

Given that Ras is a well-known oncogenic driver and Ras activity is regulated by Gal-1, we predicted that Gal-1 is a therapeutic target for MPNST. We first examined the *LGALS1* transcript levels in human NF1 from 2 Oncomine datasets of Henderson<sup>16</sup> and Nakayama,<sup>17</sup> and found that *LGALS1* was significantly higher in neurofibroma and MPNST (Fig. 1A). It has been known that loss of *NF1* is associated with activation of RAS/MAPK signaling in NF1 patients.<sup>18</sup> Overexpression of *CXCR4* has been reported in NF1 patients.<sup>13</sup> As expected, downregulation of *NF1* and upregulation of *CXCR4* were observed in NF1 patients of these 2 datasets. In addition, the protein expression level of Gal-1 was detected in human normal nerve tissue, neurofibroma, and MPNST. Significantly higher level of Gal-1 expression was observed in MPNST compared with normal nerve tissue and neurofibroma (all *P*  $< 0.001$ ; Fig. 1B), as determined by 2-tailed Student's *t*-test.

### Effects of Depletion of Gal-1 in MPNST Cells

NF96.2 (*NF1*<sup>-/-</sup>) and NF02.2 (*NF1*<sup>+/-</sup>) MPNST cell lines with endogenous Gal-1 expression were chosen for further elucidation of Gal-1 function in MPNST (Fig. 2A, B). NF96.2 and NF2.2 MPNST cells were transfected with siRNA against Gal-1, and as expected, expression of Gal-1 was found to be reduced as evaluated by western blot (Fig. 2B). In addition, knockdown Gal-1 was able to reduce cell growth (Fig. 2C) and induce apoptotic membrane blebbing (Fig. 2D) and caspase activity (Fig. 2E). SiGal-1-mediated apoptosis was further confirmed by using annexin-V to detect membrane surface phosphatidylserine, an earlier event of apoptosis (Supplementary Fig. 1A). These results indicate that Gal-1 knockdown can reduce MPNST cell viability and induce apoptosis.

### Gal-1 Knockdown Exhibits Antitumor Activity In Vivo

We next evaluated the effects of Gal-1 knockdown on MPNST tumor growth. Before in vivo testing, we performed

colony formation assay. This anchorage-independent growth assay is believed to be a good predictor of in vivo activity. Stable knockdown of Gal-1 was generated by transfection of shRNA plasmid targeting Gal-1. Knockdown Gal-1 using shGal-1 plasmid also impaired *NF1*<sup>-/-</sup> NF96.2 cell growth (Fig. 3A and Supplementary Fig. 2A). NF96.2 cells formed colonies after 2 weeks (Fig. 3B). In contrast, Gal-1 knockdown in NF96.2 cells exhibited significant inhibition in colony formation (Fig. 3B and Supplementary Fig. 2B). To examine Gal-1-mediated tumorigenicity in vivo, NF96.2 luciferase-tagged cells expressing control shRNA or shGal-1 were subcutaneously injected into nude mice. In vivo tumorigenesis studies showed that Gal-1 knockdown significantly suppressed tumor growth in nude mice (Fig. 3C, D). The xenografts were excised and weighed at the end of the experiment to confirm in vivo bioluminescence imaging results (Fig. 3E). This finding strongly suggests an oncogenic role of Gal-1 in MPNST development.

### Ras Signaling Was Inhibited by Gal-1 Knockdown

Gal-1 is known to stabilize activated Ras at the plasma membrane,<sup>9,19</sup> which was also observed in MPNST cells (Fig. 4A and Supplementary Fig. 3). The RAS pathway is frequently activated in MPNST.<sup>10-12</sup> Given that Gal-1 is essential to stabilize membrane Ras and thereby induce the activation of Ras,<sup>9</sup> we examined whether Gal-1 knockdown could have an effect on the Ras signaling pathway. We utilized a Ras pull-down activation assay to determine activated Ras level. We also assessed the expression level of CXCR4, phosphorylated MEK, and phosphorylated ERK, all of which are important therapeutic targets in cancers. Knockdown of Gal-1 with shRNA resulted in a significant decrease in expression of active Ras (Fig. 4B), CXCR4 (Fig. 4C), and reduced phosphorylation of MEK and ERK in NF96.2 and NF2.2 cells (Fig. 4D). To further confirm whether Gal-1 knockdown suppressed MPNST cell proliferation and induced apoptosis by downregulating Ras and CXCR4, pcDNA-H-Ras(G12V) or pcDNA-CXCR4 vector and shGal-1 plasmid were co-transfected into NF96.2 or NF2.2 cells (Fig. 4B, C). Restoration of H-Ras(G12V) or CXCR4 was found to inhibit apoptosis and cell death in Gal-1 shRNA transfected cells (Fig. 4E, F). Together, these data strongly indicate that Gal-1 knockdown leads to suppression of the CXCR4 and Ras/ERK pathways, thereby inhibiting cancer cell proliferation.

### Pharmacological Inhibition of Gal-1 with LLS2 in MPNST Cells

The strong growth inhibitory effects of Gal-1 specific siRNA on MPNST cells suggest that Gal-1 is an excellent therapeutic target for NF1. LLS2, a novel small-molecule inhibitor against Gal-1, identified from screening the one-bead two-compound combinatorial library, was recently demonstrated in our laboratory to be effective against ovarian cancer SKOV3 xenograft models.<sup>14</sup> Here we tested whether LLS2 exerts similar antitumor effects against MPNST cells. We found that LLS2 is indeed cytotoxic against NF96.2 and NF2.2 cells, with half-maximal

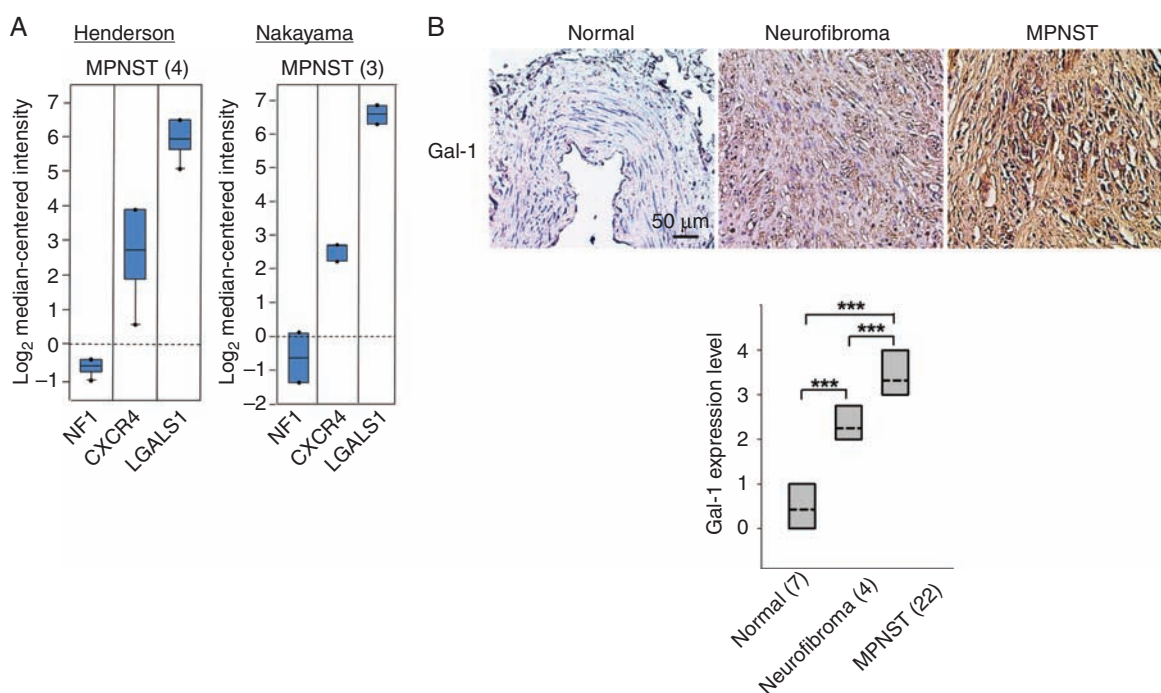


**Fig. 1** Gal-1 expression in human MPNST. (A) *NF1*, *CXCR4*, and *LGALS1* transcript levels from 2 OncoPrint datasets. Henderson, MPNST, 4 patients<sup>16</sup>; Nakayama, MPNST, 3 patients.<sup>17</sup> Data, representative units according to OncoPrint output. (B) The expression levels of Gal-1 were evaluated by immunohistochemistry (magnification, x400). Gal-1 expression in 7, 4, and 22 samples of normal nerve tissue, neurofibroma, and MPNST, respectively. Gal-1 expression was scored and displayed by boxplot (dashed line: mean; lines above and below the dashed line, third quartile to the first quartile). \*\*\* $P < 0.001$ ; 2-tailed Student's *t*-test.

inhibitory concentration values of 21.3 and 31.2  $\mu\text{M}$ , respectively (Fig. 5A). In addition, LLS2 was found to be able to induce apoptosis (Fig. 5B, Supplementary Fig. 1B) and suppress colony formation in these MPNST cells (Fig. 5C). Treatment with LLS2 at 25  $\mu\text{M}$  for 24 h recapitulated siGal-1-mediated reduction of active Ras, CXCR4, phospho-MEK, and phospho-ERK in NF96.2 and NF2.2 cells (Fig. 5D, E).

### LLS2 Has Antitumor Activity in an *NF1*<sup>-/-</sup> NF96.2 Xenograft Model

We further evaluated the effects of LLS2 on MPNST tumor growth. We implanted NF96.2 cells into nude mice via subcutaneous injection. Tumors were excised and weighed at the end of the experiment. Mice bearing the *NF1*<sup>-/-</sup> NF96.2 cells were treated with LLS2 (25 mg/kg i.v. for 5 successive days when tumors reached 75 mm<sup>3</sup>). LLS2 significantly reduced NF96.2 tumor growth ( $P < 0.001$ ; Fig. 6A–C); mean tumor volume was 238.2 mm<sup>3</sup> for the LLS2-treated group compared with 1141.1 mm<sup>3</sup> for the control group. No adverse effects such as weight loss were observed in any treated mice. To consider the aggressive nature of MPNST, a lung metastasis model was established to evaluate the metastasis-inhibitory effect of LLS2. Luciferase-tagged NF96.2 cells were tail-vein injected and treated with LLS2 (15 mg/kg i.v.) at week 3 for 5 days. Bioluminescence was used to follow the tumor burden over time. As shown in Fig. 6D, at 12 weeks, no sign of tumor

was detected in the LLS2 treated mice. In contrast, significant tumor burden was observed in control mice treated with vehicle. These studies clearly demonstrate the therapeutic efficacy of LLS2 in inhibiting both primary tumor growth and metastasis in vivo.

## Discussion

In this study, we present our discovery of the oncogenic role of Gal-1 and the tumor suppressive effects of LLS2, a benzimidazole small-molecule Gal-1 inhibitor, in MPNST. Gal-1 is overexpressed in *NF1*-associated MPNST patients. Inhibition of Gal-1 in MPNST cells via either siRNA-mediated knockdown or LLS2 treatment resulted in a decrease in expression of CXCR4 and active Ras, leading to the suppression of the downstream MEK-ERK signaling pathway (Fig. 4). From these important findings across clinical and in vitro models, we provide the first evidence that aberrant RAS activation is regulated by Gal-1 in MPNST.

*NF1* is a common genetic disorder caused by defects in the gene *NF1* encoding protein neurofibromin. *NF1* functions in part as a Ras GTPase-activating protein (GAP), converting active Ras-GTP to inactive Ras-GDP.<sup>20</sup> By accelerating GTP hydrolysis to GDP, neurofibromin is a negative regulator of Ras.<sup>21</sup> *NF1* mutations in neurofibromas and MPNSTs result in elevated level of active Ras-GTP.<sup>11,12</sup> Ras is initially translated on ribosomes as inactive protein, before attaching

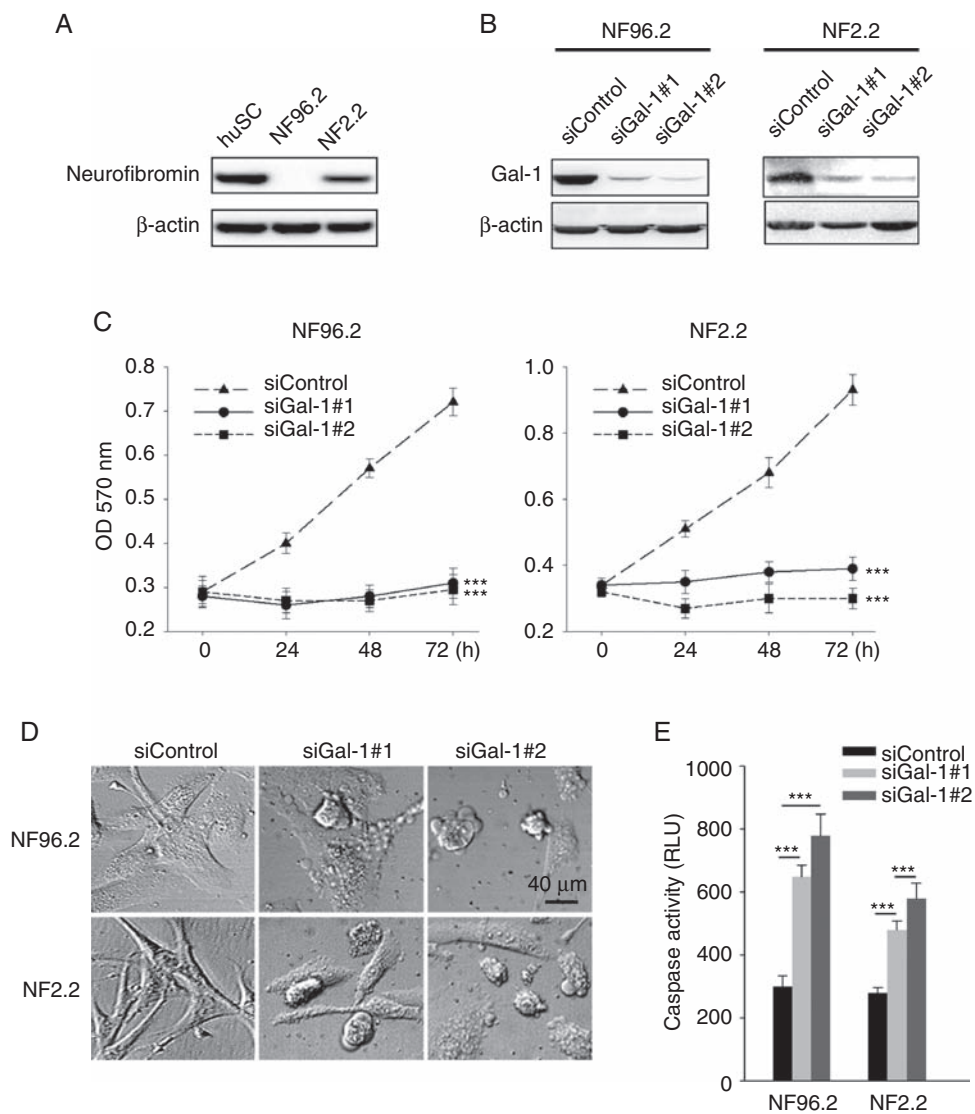


**Fig. 2** Effect of Gal-1 inhibition in MPNST cells. (A) Immunoblots demonstrate the expression of neurofibromin in normal huSC (positive control), NF96.2, and NF2.2 cells. (B) Suppression of endogenous Gal-1 expression by siRNA in *NF1*<sup>-/-</sup> NF96.2 and *NF1*<sup>+/-</sup> NF2.2 MPNST cells. (C) MPNST cells transfected with 40 nM scramble control siRNA or siRNA against Gal-1; cell survival was determined by MTT. (D) Morphology of MPNST cells 72 h after transfected with 40 nM scramble control siRNA or siRNA against Gal-1. (E) Caspase-3/7 activities in NF96.2 and NF2.2 cells 72 h after transfection with 40 nM siRNA. \*\*\**P* < 0.001; 2-tailed Student's *t*-test. Data shown are mean ± SD.

to the cell membrane after prenylation and palmitoylation.<sup>22</sup> Activated Ras at the plasma membrane is essential for induction of the oncogenic signaling pathway, and activated Ras/membrane interaction is stabilized by Gal-1. Moreover, overexpression of Gal-1 has been shown to increase membrane-associated Ras, Ras-GTP, and active ERK.<sup>9</sup> In our study, we observed that knockdown of Gal-1 decreased the expression of activated Ras, which is consistent with prior findings. Conversely, Ras inhibition by salirasib or farnesylthiosalicylic acid, a Ras farnesylcysteine mimetic, has been reported to reduce Gal-1 expression in *NF1*<sup>-/-</sup> MPNST cells.<sup>23</sup> According to these studies, upregulated Gal-1 might contribute to the oncogenicity in *NF1*<sup>-/-</sup> cells via Gal-1/Ras autocrine or paracrine pathways.

CXCR4 has been implicated as a key molecular player regulating cancer development and progression, including MPNST.<sup>13,24–26</sup> How CXCR4 is upregulated in cancers, however, remains unclear. In this study, we demonstrated that shRNA-mediated Gal-1 knockdown decreased the expression level of CXCR4, leading to the inhibition of cell growth. In addition, transfection of pcDNA-H-Ras(G12V) plasmid into Gal-1 shRNA transfected cells increased the expression of CXCR4 (Supplementary Fig. 4), suggesting that Gal-1 regulates CXCR4 expression via RAS signaling. In support of our finding, Huang et al reported that Gal-1 can regulate CXCR4 expression through ERK/nuclear factor-kappaB activation, contributing to kidney cancer progression, and suggested that a Gal-1–CXCR4 axis is a

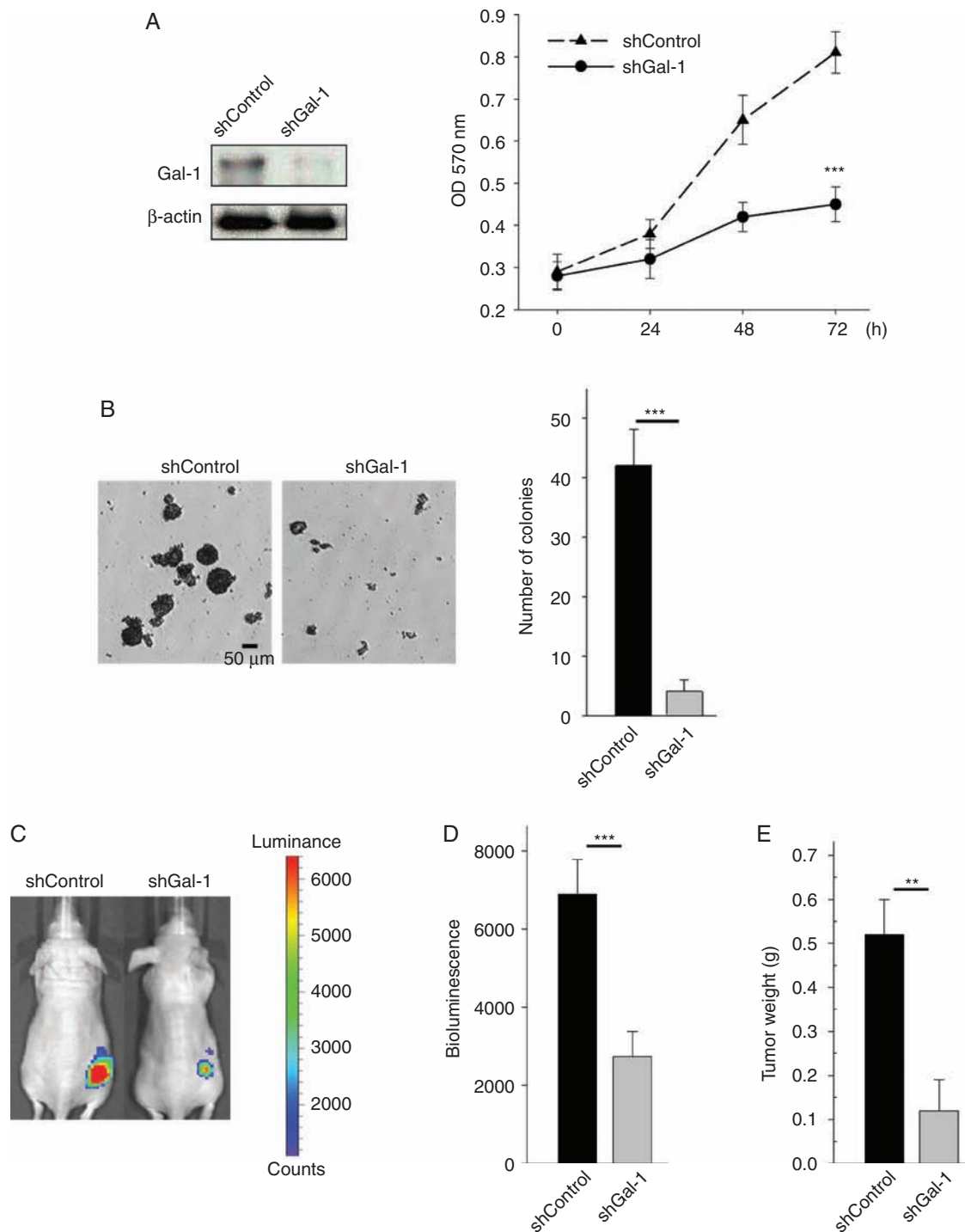


**Fig. 3** Effect of Gal-1 knockdown in *NF1*<sup>-/-</sup> NF96.2 xenograft model. (A) Suppression of endogenous Gal-1 expression by shRNA in NF96.2 cells, and cell proliferation was measured. (B) Colony formation on NF96.2 cells and quantification of colony number larger than 50  $\mu$ m after 2 weeks. (C) Bioluminescent images show the growth of subcutaneously implanted luciferase-tagged NF96.2 cells (stably transfected with shRNA or Gal-1 shRNA) in nude mice on week 14 ( $n = 6$  mice per group). (D) Quantification of the tumor bioluminescent signal. (E) Weight of the tumor xenografts. \*\* $P < 0.01$ , \*\*\* $P < 0.001$ ; 2-tailed Student's  $t$ -test. Data shown are mean  $\pm$  SD.

therapeutic target for kidney cancer.<sup>27</sup> Thus, Gal-1-targeted therapy leading to dual suppression of CXCR4 and Ras signaling is a potential strategy for the treatment of MPNST.

It is known that Gal-1 binds to oncogenic H-Ras and activates the ERK signaling pathway, resulting in cell transformation.<sup>9</sup> Interestingly, low Gal-1 expression was also observed in plexiform neurofibroma (Fig. 1B). Based on these clinical



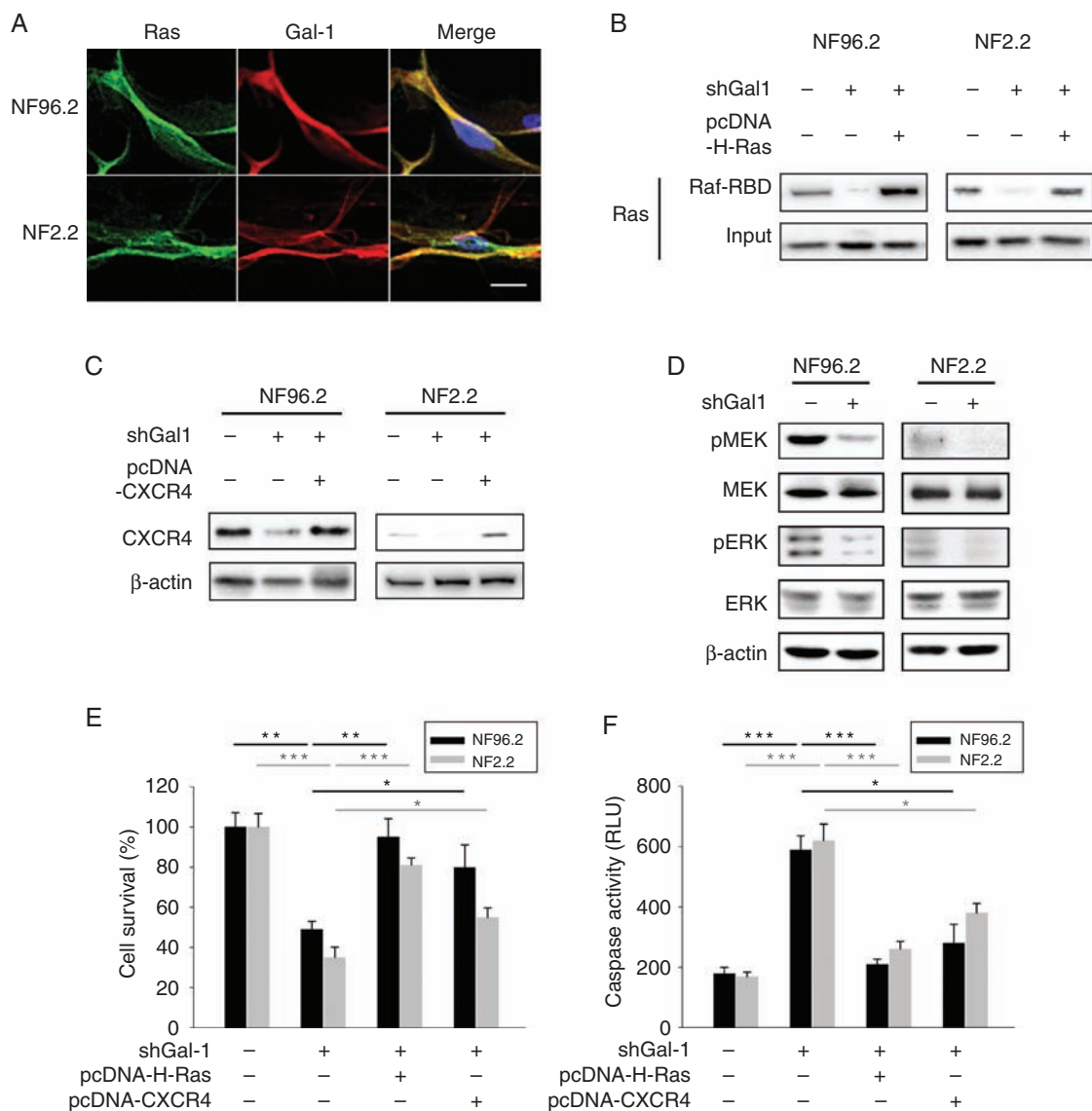


**Fig. 4** Effect of Gal-1 knockdown on Ras pathways in MPNST cells. (A) Co-localization of Gal-1 and Ras. (B) Active Ras pull-down assay. NF96.2 and NF2.2 cells were co-transfected with 1.5  $\mu$ g shControl or shGal-1, and 1  $\mu$ g pcDNA or pcDNA-H-Ras(G12V). Seventy-two hours post-transfection, cell lysates were extracted and incubated with Raf-1 RBD agarose. Input: total protein extracted from MPNST cells were not incubated with Raf-1 RBD agarose. Eluted proteins were analyzed by SDS-PAGE and immunoblotted with anti-RAS antibodies. (C) CXCR4 was examined by immunoblotting after 72 h post-transfection with control shRNA or shGal-1, and pcDNA or pcDNA-CXCR4. (D) Immunoblotting of phospho-MEK, MEK, phospho-ERK, and ERK in NF96.2 and NF2.2 transfected with 1  $\mu$ g control shRNA or shGal-1 for 72 h. (E) NF96.2 and NF2.2 cells were co-transfected with 1  $\mu$ g control shRNA or shGal-1, and 1  $\mu$ g pcDNA or pcDNA-H-Ras(G12V) or pcDNA-CXCR4; cell survival and (F) caspase-3/7 activities were measured at 72 h after transfection. \* $P < 0.05$ . \*\* $P < 0.01$ . \*\*\* $P < 0.001$ : 2-tailed Student's *t*-test. Data shown are mean  $\pm$  SD. Scale bars, 20  $\mu$ m.

observations, we hypothesized that Gal-1 expression in plexiform neurofibroma is involved in malignant transformation and that inhibition of Gal-1 function may prevent or abrogate progression of plexiform neurofibroma into MPNST. Further studies to investigate the malignant transformation effects of Gal-1 in plexiform neurofibroma are currently ongoing.

The Ras signaling pathway is frequently dysregulated in MPNST. Understanding the molecular mechanisms in control of Ras-related signaling pathways is important for the development of new rational therapies against this disease.

Lonafarnib is a potent orally administered farnesyl transferase inhibitor (FTI) that interferes with Ras prenylation and palmitoylation.<sup>28</sup> It is under clinical development for the treatment of progeria and various types of cancer, including glioma, glioblastoma, and breast cancer.<sup>29-31</sup> Another FTI that produced promising results in clinical trial is tipifarnib.<sup>32</sup> Downstream effectors of Ras, including Raf, MAPK, and ERK, are also critical for Ras signaling. Some compounds that inhibit these molecular targets have entered clinical trials in various cancer types. For example, binimetinib,

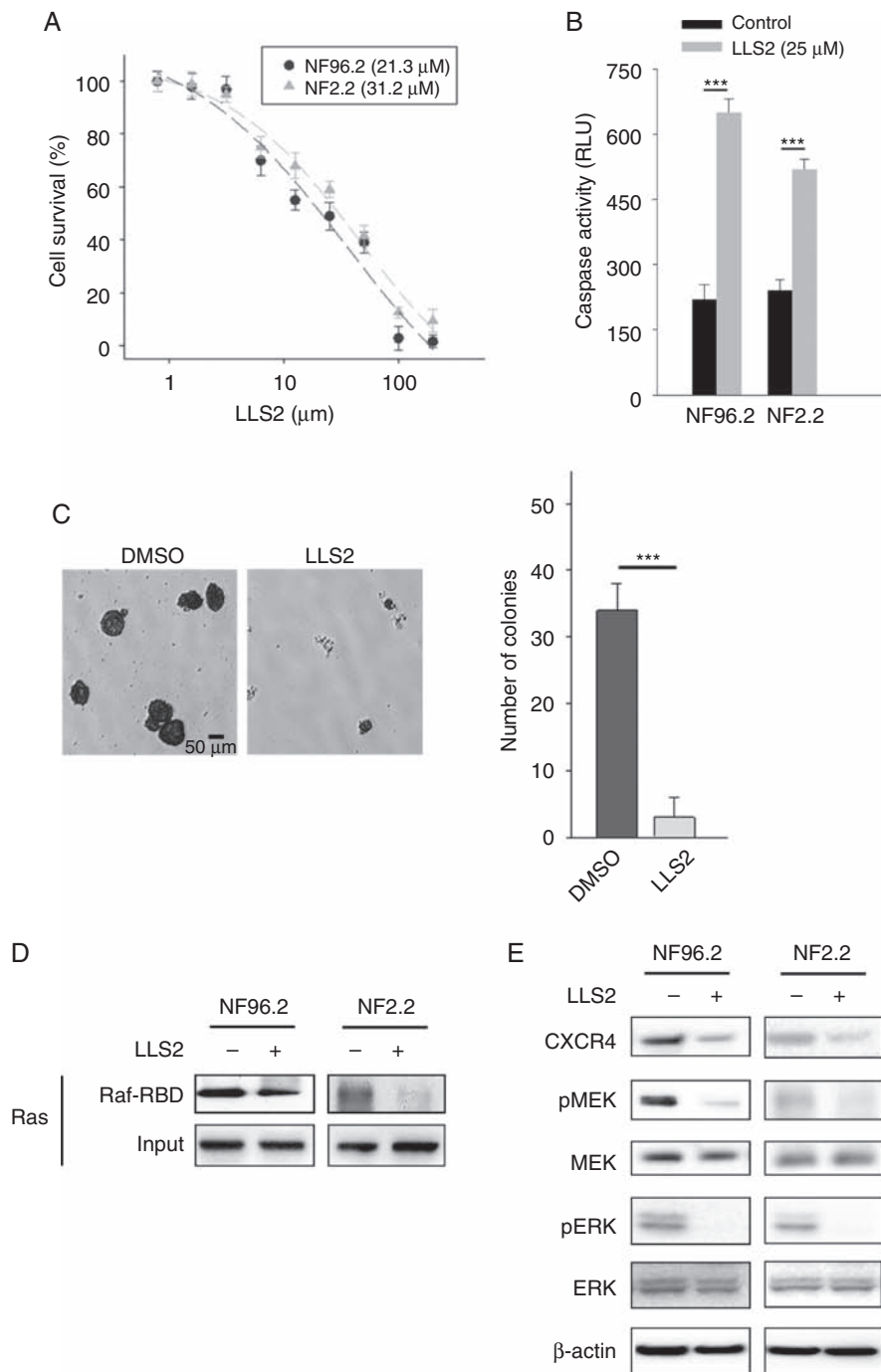


**Fig. 5** The therapeutic efficacy of LLS2 against MPNST cells. (A) Cell survival of NF96.2 and NF2.2 MPNST cells treated with indicated concentrations of LLS2 for 72 h. Half-maximal inhibitory concentrations of LLS2 on NF96.2 and NF2.2 are 21.3  $\mu$ M and 31.2  $\mu$ M, respectively. (B) Caspase-3/7 activities in NF96.2 and NF2.2 cells after 24 h treated with 0.25% DMSO or 25  $\mu$ M LLS2 (C) Representative images and quantification of colony formation. (D) Active Ras pull-down assay. MPNST cells were treated with 0.25% DMSO or 25  $\mu$ M LLS2, and cell lysates were prepared at 24 h, followed by incubating with Raf-1 RBD agarose. Input: total protein extracted from MPNST cells were not incubated with Raf-1 RBD agarose. Eluted proteins were analyzed by SDS-PAGE and immunoblotted with RAS antibodies. (E) Immunoblots of CXCR4, phospho-MEK, MEK, phospho-ERK, and ERK in NF96.2 and NF2.2 treated with vehicle control 0.25 % DMSO or 25  $\mu$ M LLS2 for 24 h. \*\*\* $P < 0.001$ ; 2-tailed Student's  $t$ -test. Data shown are mean  $\pm$  SD.

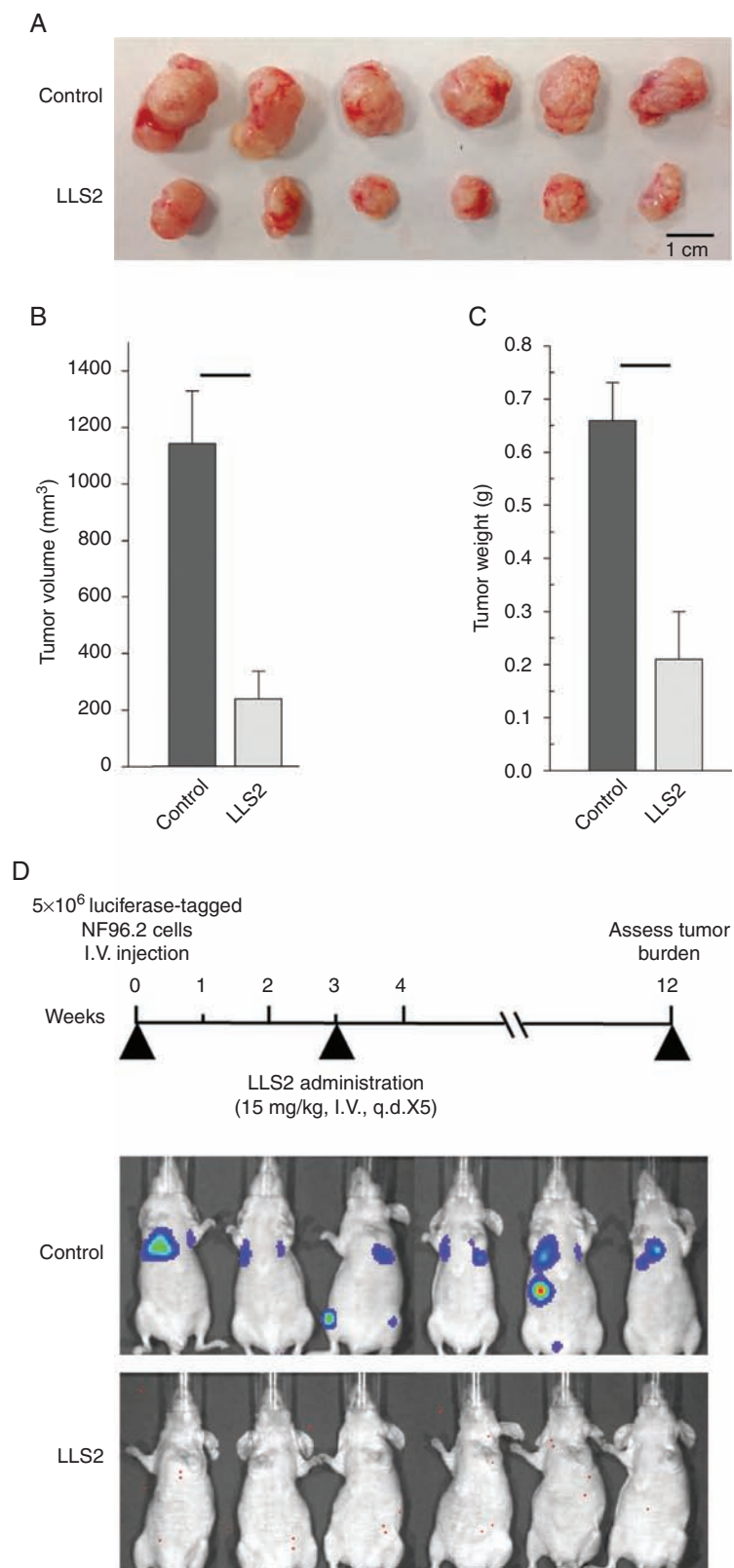


**Fig. 6** LLS2 have antitumor activity in *NF1*<sup>-/-</sup> NF96.2 xenograft model. (A) Xenograft tumors. (B) Volume and (C) weight of the tumor xenografts were measured at 3 weeks after treatment. (D) Timeline of LLS2 treatment protocol; bioluminescent images for vehicle (8.7% alcohol/8.7% cremophor) or LLS2 treated mice were obtained at 12 weeks after initial i.v. injection of NF96.2 cells. \*\**P* < 0.01, \*\*\**P* < 0.001; 2-tailed Student's *t*-test, *n* = 6. Data shown are mean ± SD.

an FDA-approved inhibitor of MEK 1 and 2, is currently undergoing phase III trials, in combination with other drugs. Binimetinib in combination with encorafenib (a B-raf inhibitor) is being evaluated in advanced melanoma (National Cancer Institute, NLM# NCT01909453). Combination encorafenib, binimetinib, and cetuximab (an anti-epidermal growth factor receptor antibody) is being evaluated in patients with advanced colorectal cancer (National Cancer Institute, NLM# NCT02928224). These promising Ras pathway inhibitors may have great therapeutic potential against MPNST. LLS2 inhibits the Ras pathway via a mechanism totally different from that of the above-mentioned drugs. It is conceivable that LLS2 may potentiate the therapeutic effects of these drugs, not only against MPNST, but also against a variety of cancers such as melanoma, colon cancer, and pancreatic cancer. Work is currently under way in our laboratory to explore these possibilities.

## Supplementary Material

Supplementary data are available at *Neuro-Oncology* online.

## Keywords

CXCR4 | galectin-1 | LLS2 | MPNST | RAS

## Funding

This work was supported by National Institutes of Health R33 CA160132 and R01CA115483 to K.S.L.

## Acknowledgments

We thank Dr Marcio Malogolowkin and Dr Ruben Antony for valuable input on an earlier version of the manuscript. We also thank Tissue Bank at Chang Gung Memorial Hospital, Keelung for technical support of tissue staining.

**Conflict of interest statement.** T. Shih, R. Liu, and K. S. Lam are the inventors of a pending patent on LLS2. The remaining authors declare no potential conflicts of interests.

**Authorship statement: Conception and design:** T. Shih, K. Lam. **Development of methodology:** T. Shih, Y. Fan, X. Li, S. Kiss, X. Chen, P. Ghosh, K. Lam. **Acquisition of data:** T. Shih, X. Li, S. Kiss, X. Deng, A. Chen, X. Chen. **Analysis and interpretation of data:** T. Shih, Y. Fan, X. Li, X. Chen, R. Carney, K. Lam. **Writing, review of the manuscript:** T. Shih, R. Carney, K. Lam. **LLS2 synthesis:** R. Liu.

## References

1. Ferner RE. Neurofibromatosis 1. *Eur J Hum Genet.* 2007;15(2):131–138.
2. Huson SM, Acosta MT, Belzberg A, et al. Back to the future: proceedings from the 2010 NF conference. *Am J Med Genet A.* 2011;155A(2):307–321.
3. Zhang P, Zhang P, Shi B, et al. Galectin-1 overexpression promotes progression and chemoresistance to cisplatin in epithelial ovarian cancer. *Cell Death Dis.* 2014;5:e991.
4. Van den Brûle FA, Waltregny D, Castronovo V. Increased expression of galectin-1 in carcinoma-associated stroma predicts poor outcome in prostate carcinoma patients. *J. Pathol.* 2001;193(1):80–87. <https://onlinelibrary.wiley.com/doi/abs/10.1002/1096-9896%282000%299999%3A9999%3C%3A%3A%3AID-PATH730%3E3.0.CO%3B2-2>
5. Carlini MJ, Roitman P, Nuñez M, et al. Clinical relevance of galectin-1 expression in non-small cell lung cancer patients. *Lung Cancer.* 2014;84(1):73–78.
6. Jung EJ, Moon HG, Cho BI, et al. Galectin-1 expression in cancer-associated stromal cells correlates tumor invasiveness and tumor progression in breast cancer. *Int J Cancer.* 2007;120(11):2331–2338.
7. White NM, Masui O, Newsted D, et al. Galectin-1 has potential prognostic significance and is implicated in clear cell renal cell carcinoma progression through the HIF/mTOR signaling axis. *Br J Cancer.* 2014;110(5):1250–1259.
8. Martínez-Bosch N, Fernández-Barrena MG, Moreno M, et al. Galectin-1 drives pancreatic carcinogenesis through stroma remodeling and Hedgehog signaling activation. *Cancer Res.* 2014;74(13):3512–3524.
9. Paz A, Haklai R, Elad-Sfadia G, Ballan E, Kloog Y. Galectin-1 binds oncogenic H-Ras to mediate Ras membrane anchorage and cell transformation. *Oncogene.* 2001;20(51):7486–7493.
10. De Raedt T, Maertens O, Chmara M, et al. Somatic loss of wild type NF1 allele in neurofibromas: comparison of NF1 microdeletion and non-microdeletion patients. *Genes Chromosomes Cancer.* 2006;45(10):893–904.
11. Basu TN, Gutmann DH, Fletcher JA, Glover TW, Collins FS, Downward J. Aberrant regulation of ras proteins in malignant tumour cells from type 1 neurofibromatosis patients. *Nature.* 1992;356(6371):713–715.
12. Sherman LS, Atit R, Rosenbaum T, Cox AD, Ratner N. Single cell Ras-GTP analysis reveals altered Ras activity in a subpopulation of neurofibroma Schwann cells but not fibroblasts. *J Biol Chem.* 2000;275(39):30740–30745.
13. Mo W, Chen J, Patel A, et al. CXCR4/CXCL12 mediate autocrine cell-cycle progression in NF1-associated malignant peripheral nerve sheath tumors. *Cell.* 2013;152(5):1077–1090.
14. Shih TC, Liu R, Fung G, Bhardwaj G, Ghosh PM, Lam KS. A novel Galectin-1 inhibitor discovered through one-bead two-compound library potentiates the antitumor effects of paclitaxel in vivo. *Mol Cancer Ther.* 2017;16(7):1212–1223.
15. Shih TC, Liu R, Wu CT, et al. Targeting Galectin-1 impairs castration-resistant prostate cancer progression and invasion. *Clin Cancer Res.* 2018;24(17):4319–4331.
16. Henderson SR, Guiliano D, Presneau N, et al. A molecular map of mesenchymal tumors. *Genome Biol.* 2005;6(9):R76.
17. Nakayama R, Nemoto T, Takahashi H, et al. Gene expression analysis of soft tissue sarcomas: characterization and reclassification of malignant fibrous histiocytoma. *Mod Pathol.* 2007;20(7):749–759.

18. Ratner N, Miller SJ. A RASopathy gene commonly mutated in cancer: the neurofibromatosis type 1 tumour suppressor. *Nat Rev Cancer*. 2015;15(5):290–301.
19. Julie E, Thuy N, Douglas C, Lotan Dafna, Reuben L. Differential expression of endogenous galectin-1 and galectin-3 in human prostate cancer cell lines and effects of overexpressing galectin-1 on cell phenotype. *Int J Oncol*. 1999;14(2):217–224.
20. DeClue JE, Cohen BD, Lowy DR. Identification and characterization of the neurofibromatosis type 1 protein product. *Proc Natl Acad Sci U S A*. 1991;88(22):9914–9918.
21. Phillips RA, Hunter JL, Eccleston JF, Webb MR. The mechanism of Ras GTPase activation by neurofibromin. *Biochemistry*. 2003;42(13):3956–3965.
22. Casey PJ, Seabra MC. Protein prenyltransferases. *J Biol Chem*. 1996;271(10):5289–5292.
23. Barkan B, Cox AD, Kloog Y. Ras inhibition boosts galectin-7 at the expense of galectin-1 to sensitize cells to apoptosis. *Oncotarget*. 2013;4(2):256–268.
24. Sleightholm RL, Neilsen BK, Li J, et al. Emerging roles of the CXCL12/CXCR4 axis in pancreatic cancer progression and therapy. *Pharmacol Ther*. 2017;179:158–170.
25. Xu C, Zhao H, Chen H, Yao Q. CXCR4 in breast cancer: oncogenic role and therapeutic targeting. *Drug Des Devel Ther*. 2015;9:4953–4964.
26. Conley-LaComb MK, Semaan L, Singareddy R, et al. Pharmacological targeting of CXCL12/CXCR4 signaling in prostate cancer bone metastasis. *Mol Cancer*. 2016;15(1):68.
27. Huang CS, Tang SJ, Chung LY, et al. Galectin-1 upregulates CXCR4 to promote tumor progression and poor outcome in kidney cancer. *J Am Soc Nephrol*. 2014;25(7):1486–1495.
28. Njoroge FG, Taveras AG, Kelly J, et al. (+)-4-[2-[4-(8-Chloro-3,10-dibromo-6,11-dihydro-5H-benzo[5,6]cyclohepta[1,2-b]pyridin-11@-yl)-1-piperidinyl]-2-oxo-ethyl]-1-piperidinecarboxamide (SCH-66336): a very potent farnesyl protein transferase inhibitor as a novel antitumor agent. *J Med Chem*. 1998;41(24):4890–4902.
29. Lo HW. Targeting Ras-RAF-ERK and its interactive pathways as a novel therapy for malignant gliomas. *Curr Cancer Drug Targets*. 2010;10(8):840–848.
30. Yust-Katz S, Liu D, Yuan Y, et al. Phase 1/1b study of lonafarnib and temozolomide in patients with recurrent or temozolomide refractory glioblastoma. *Cancer*. 2013;119(15):2747–2753.
31. Kerklaan BM, Diéras V, Le Tourneau C, et al. Phase I study of lonafarnib (SCH66336) in combination with trastuzumab plus paclitaxel in Her2/neu overexpressing breast cancer: EORTC study 16023. *Cancer Chemother Pharmacol*. 2013;71(1):53–62.
32. End DW, Smets G, Todd AV, et al. Characterization of the antitumor effects of the selective farnesyl protein transferase inhibitor R115777 *in vivo* and *in vitro*. *Cancer Res*. 2001;61(1):131–137.